SOIL, 12, 279–294, 2026
https://doi.org/10.5194/soil-12-279-2026

SOIL Open Access EGU

Leaching behavior of steelmaking slag fertilizer under repeated wetting and drying conditions simulating upland soil

Takayuki Iwama[1], **Shohei Koizumi**[2], **Megumi Obara**[1], **and Shigeru Ueda**[1]

[1]Institute of Multidisciplinary Research for Advanced Materials, Tohoku University, 2-1-1, Katahira, Aoba-ku, Sendai, 980-8577, Japan
[2]Advanced Technology Research Laboratories, Nippon Steel, 20-1, Shintomi, Futtsu, 293-8511, Japan

Correspondence: Takayuki Iwama (takayuki.iwama.a6@tohoku.ac.jp)

Received: 19 December 2025 – Discussion started: 30 December 2025
Revised: 10 March 2026 – Accepted: 20 March 2026 – Published: 26 March 2026

Abstract. To determine how steelmaking slag dissolves and modulates soil acidity and exchangeable cations under upland-like repeated wetting–drying conditions, we conducted a soil-column experiment. Specifically, we aimed to identify the Ca-supplying phases responsible for pH correction, evaluate their persistence during extended leaching, and define the layer-scale reach of the effect to inform application planning (rate, placement, and maintenance). Soil columns incorporating discrete slag-amended layers were prepared together with unamended controls. A repeated wetting–drying leaching test was run up to 24 weeks; after termination, each column was sampled by layer, and soil pH and exchangeable CaO were measured. Additionally, surfaces and cross-sections of slag particles embedded in the columns were observed to identify dissolving phases and secondary precipitates. In the control columns, soil pH remained in the acidic range (4.8–5.5), whereas slag-amended layers maintained pH 6.0–6.5 for 24 weeks in the test columns. Adjacent unamended layers in the test columns showed no detectable change, indicating that the effect was confined to the amended layers. Exchangeable CaO increased in soils mixed with slag. Microstructural observations revealed alteration and dissolution of free lime (f-CaO) and dicalcium silicate ($2\,CaO \cdot SiO_2$), with calcium carbonate ($CaCO_3$) precipitates on particle surfaces. These Ca-supplying phases persisted after 24 weeks of leaching. Sustained Ca release from f-CaO and $2\,CaO \cdot SiO_2$, together with $CaCO_3$ precipitation, produced localized, durable pH correction in slag-amended layers while leaving adjacent layers unchanged. The defined reach and persistence provide a mechanistic basis for application planning in acidic upland soils – informing rate, placement within the profile, and maintenance intervals.

1 Introduction

Steelmaking slag is a by-product generated during steel production. It is produced in the process of converting pig iron, which is obtained by reducing iron ore in a blast furnace, into tough steel by removing impurities such as carbon, phosphorus, and sulfur. The properties of steelmaking slag vary depending on the steelworks and the type of steel being produced; however, its main components typically include Ca, Si, Fe, Mg, Mn, and P, all of which are beneficial to plant growth (Nippon Slag Association, 2015). Steelmaking slag is primarily used as a fertilizer material in paddy fields. It supplies silica to rice plants, which strengthens their resistance to lodging, high temperatures, and pests (Ahire et al., 2021; Verma et al., 2024). It also helps suppress reductive conditions in paddy soils by replenishing iron and manganese that leach out, thereby preventing "aki-ochi" – a decline in rice yield caused by hydrogen sulfide generation (Shiratori, 2024). In addition, controlling methane emissions, which are released as a result of reduction processes occurring in paddy soils (Appelo and Postma, 2004), has become an important goal for sustainable rice farming, and slag use is expected to contribute to the reduction of greenhouse gas emissions (Ito,

2015; Inubushi et al., 2018; Inubushi, 2021; Yamamoto and Morii, 2020).

Steelmaking slag fertilizers are also beneficial in upland fields. When applied for soil pH correction, it can raise soil pH to weakly alkaline levels without leading to growth inhibition associated with micronutrient deficiencies. Soil pH has been raised to around 7.5 as a means of suppressing soil-borne diseases such as clubroot in Brassica crops and bacterial wilt in tomatoes (NARO, 2015). Moreover, the effect of steelmaking slag fertilizer in improving soil pH has been reported to last longer than that of conventional liming materials such as calcium carbonate (Goto, 2016), making it possible to maintain the effect over an extended period with a single application.

Steelmaking slag also contains phosphate, one of the three essential nutrients for stable food production. Although the P_2O_5 content in slag ranges from 2 mass % to 10 mass % (Matsubae-Yokoyama et al., 2009) and is lower than that in conventional phosphate fertilizers such as fused phosphate or superphosphate (Food and Agriculture Materials Inspection Center, 2024), Japan, which is one of the world's largest steel producers, generates approximately 12 million t of steelmaking slag annually (Nippon Slag Association, 2024). Assuming a P_2O_5 concentration of 3.5 mass %, the total phosphorus contained in slag corresponds to Japan's annual phosphorus imports (JOGMEC, 2021). In recent years, the importance of exploring underutilized domestic resources that contain N, P, and K has increasingly been recognized for the sustainability and stability of agriculture, further enhancing the value of steelmaking slag as a fertilizer material.

To meet this growing demand, it is necessary to clarify the amount and rate of nutrient release from steelmaking slag fertilizers into soil, which is essential for integrating slag into broader fertilization strategies. Various leaching tests have been conducted in paddy environments, mainly focusing on the supply of silica (Gao et al., 2015; Ito, 2022; Maruoka et al., 2015; Okubo et al., 2015). For example, it has been reported that the amount of silica actually absorbed by rice plants is better predicted not by total silicon content or the amount extractable with 0.5 mol L^{-1} HCl, but rather by the plant-available silica extractable in near-neutral solutions such as tris buffer (Furuzono et al., 2022). Moreover, studies involving slag embedded in actual paddy soils and analyzed via cross-sectional observation (Ito et al., 2015; Ito, 2022) have shown that larnite ($2\,CaO \cdot SiO_2$) is the main source of plant-available silica in weakly acidic to neutral conditions, and that there are significant differences in silica supply ability among various silicate minerals in slag.

Studies on the use of steelmaking slag fertilizer in upland fields have mainly focused on how changes in soil pH caused by slag application affect crop yield, nutrient uptake, or the incidence of soil-borne diseases (Deus et al., 2020; Iwadate, 2017; Murakami and Goto, 2006; Sinegovskaya et al., 2020). However, there is limited research on the specific dissolution behavior of slag in upland soils. Soil acidification can markedly reduce crop yields. One material widely used to correct soil pH is limestone. Limestone improves soil acidity by consuming H^+ during dissolution and the formation of HCO_3^- and $CO_2 + H_2O$ (Oliveira and Pavan, 1996; Caires et al., 2003; Holland et al., 2018). Calcium silicate has a higher solubility than limestone (approximately 6–7 times) and has been studied as an alternative liming material (Amoakwah et al., 2023). The acidity-correction mechanism of silicate is similar to that of limestone: SiO_3^{2-} released during dissolution is supplied to the soil and mitigates acidity by binding with H^+ (Alcarde and Rodella, 2003). Other materials have also been studied, including highly reactive dolomitic limestone containing Mg (Castro et al., 2011), calcium magnesium silicate (Castro et al., 2011), and materials with high neutralizing value such as quicklime/burnt lime and slaked lime (Goulding, 2016; Holland et al., 2018).

Steelmaking slag consists of multiple mineral phases including reactive phases such as $2\,CaO \cdot SiO_2$, tricalcium silicate ($3\,CaO \cdot SiO_2$), and lime phase (CaO) (Das et al., 2007). Similar to other alkaline amendments, its capacity to mitigate soil acidity is based on dissolution of these phases and consumption of H^+ by the released anions. Compared with limestone and silicate, steelmaking slag has been reported to provide comparable pH-correction capacity and improvements in soybean yield (Deus et al., 2020). Thus, steelmaking slag can be a valuable material for agricultural use in terms of yield improvement.

On the other hand, concerns remain regarding the leaching and potential contamination by heavy metals. This issue has been continuously investigated, and many studies report limited impacts under certain conditions. For example, Deus et al. (2020) showed that soil Cd, Pb, and Ni contents 23 months after steelmaking slag application were almost unchanged from the control, and that Cr, Hg, Cd, and Pb were not detected in crop tissues. In steelmaking slags produced in the blast furnace–basic oxygen furnace route, the primary potentially problematic elements originating from the ore are Cr and V. The European Commission – led SLAGFERTILISER project reported that increases in soil Cr and V 3 years after slag application were small (EU, 2017). Pistocchi et al. (2017) reported that, although V and Cr did not accumulate in tomato fruits after slag application, an increasing trend in soil accumulation was observed, indicating the need to manage application rates.

In Japan, field studies have also evaluated the effects of steelmaking slag fertilizer, reporting reduced disease incidence and improved yields, while no accumulation of heavy metals in plant tissues was observed (NARO, 2015). Proposed mechanisms for limited heavy-metal impacts include the formation of sparingly soluble heavy-metal hydroxides as soil pH increases and adsorption of heavy-metal ions onto the surfaces of secondary reaction products. Therefore, steelmaking slag fertilizer, which can maintain elevated soil pH over long periods, may also be beneficial for immobilizing not only heavy metals potentially associated with the amend-

ment itself but also heavy metals originally present in the soil.

Unlike paddy soils, which are saturated with water and exist under reducing conditions due to limited oxygen supply (Maruoka et al., 2015), upland soils experience alternating wet and dry cycles and are exposed to atmospheric oxygen, resulting in oxidative conditions. These environmental differences suggest that the dissolution behavior of slag fertilizer would differ significantly between paddy and upland conditions. In upland farming, the primary expected benefit of steelmaking slag fertilizer is its ability to increase soil pH, attributed to its alkaline components, such as Ca^{2+} and Mg^{2+}. However, the alkaline components in slag exist in various mineral forms, including not only CaO, portlandite ($Ca(OH)_2$), and calcite ($CaCO_3$) as found in typical liming agents, but also $2\,CaO \cdot SiO_2$, srebrodolskite ($2\,CaO \cdot Fe_2O_3$), åkermanite ($Ca_2MgSi_2O_7$), and gehlenite ($Ca_2Al_2SiO_7$) (Gao et al., 2015; Ito et al., 2015). Understanding how each of these mineral phases dissolves is crucial for designing effective fertilizer application strategies aimed at improving soil pH. In addition, understanding how phosphorus, iron, manganese, and other micronutrients dissolve is important for realizing the full potential of steelmaking slag as a fertilizer.

In conventional research approaches, the persistence of fertilizer and alkaline amendment effects is often assessed through periodic soil sampling and measurement after application. Because the effects of fertilizers and various amendments arise from complex rhizosphere interactions involving soil, rainfall conditions, and crops, validation under actual field conditions is essential. However, approaches that depend on post-application monitoring are insufficient for the predictive quantification of fertilizer depletion rates and their use in fertilizer management planning. Therefore, this study investigates how steelmaking slag fertilizer dissolves under conditions simulating upland field environments, and evaluates its effects on soil pH, exchangeable cations, and plant-available phosphorus. The same observational scheme can provide a common basis when comparing fertilizer behavior across products under identical hydrologic forcing.

2 Experimental

2.1 Samples

The soil used in this study was Andosol, which accounts for approximately 45.1 % of Japan's land area and is widely used in agricultural fields (Saigusa and Matsuyama, 1998). The test soil had a gravimetric water content of 41 % on a dry weight basis. A commercially available fertilizer was used, which is produced by pulverizing steelmaking slag. This slag fertilizer does not exhibit heavy-metal leaching, in accordance with the guidelines established by the Nippon Slag Association (2026). The chemical composition of the slag fertilizer is shown in Table 1. The elemental composition was determined by digesting the slag sample in a mixture of hydrochloric acid, nitric acid, and hydrofluoric acid, followed by analysis of the solution using inductively coupled plasma–atomic emission spectroscopy (ICP–AES). The concentrations of each element were converted to their corresponding oxide forms (Fe was expressed as FeO). The category labeled "Others" is presumed to represent H_2O and CO_2 that reacted with the slag fertilizer.

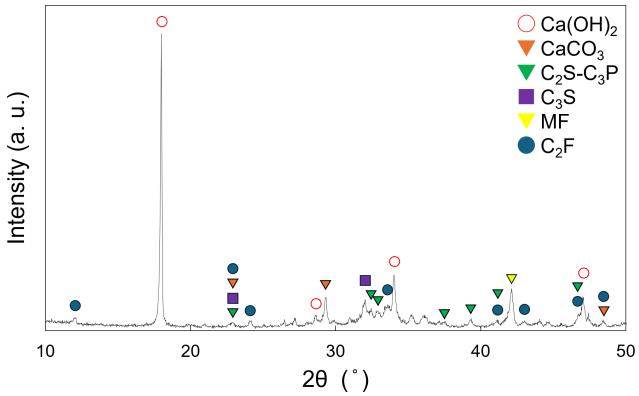

Figure 1. XRD pattern of slag fertilizer.

The X-ray diffraction (XRD) pattern of the slag fertilizer is shown in Fig. 1. Diffraction peaks corresponding to calcium hydroxide ($Ca(OH)_2$), calcium carbonate ($CaCO_3$), dicalcium silicate ($2\,CaO \cdot SiO_2$; C_2S), tricalcium silicate ($3\,CaO \cdot SiO_2$; C_3S), magnesiowüstite (MgO–FeO solid solution; MF), and dicalcium ferrite ($2\,CaO \cdot Fe_2O_3$; C_2F) were identified, indicating that the slag fertilizer consists of multiple mineral phases. These mineral phases are commonly found in typical steelmaking slag (Gao et al., 2015; Gu et al., 2025; Li et al., 2024; Matsui, 2020), and the slag fertilizer used in this study is not a specialized product, but one derived from general blast furnace–basic oxygen furnace (BF–BOF) process slag.

2.2 Experimental apparatus

A schematic of the experimental apparatus is shown in Fig. 2. To simulate upland soil conditions, including evaporation from the soil surface and downward water infiltration, a soil column apparatus was constructed using the following procedure: A rigid polyvinyl chloride (PVC) cylinder (inner diameter: 52 mm; length: 500 mm) was used. One end of the cylinder was sealed with a silicone rubber stopper containing a 10 mm diameter hole at its center. A vinyl hose (outer diameter: 10 mm; inner diameter: 8 mm; length: 50 mm) was inserted into the hole to allow water drainage. A piece of gauze (diameter: 40 mm, aperture size: 1.07 mm × 0.47 mm) was placed over the rubber stopper from the open end of the column to prevent soil loss. To build the base soil layers, 85 g of the test soil was packed into the column while tapping to ensure uniform compaction, forming a layer approximately

Table 1. Chemical composition of steelmaking slag fertilizer.

Mass %								mg kg^{-1}	
CaO	Others	FeO	MgO	MnO	Al_2O_3	P_2O_5	Others	Cr	V
40.9	13.5	21.4	6.6	2.1	3.0	1.8	13.2	2020	990

5 cm thick. A plastic mesh (diameter: 52 mm, maximum inscribed-circle diameter: 0.28 mm) was then placed on top of the soil. This process was repeated two more times to build a total of three soil layers, with plastic mesh inserted between each layer to separate them for post-experiment sampling. Next, three layers of a soil–slag mixture were prepared, each consisting of 85 g of soil and 1 g of slag fertilizer powder that passed through a 212 µm sieve (hereafter referred to as the soil–slag mixture). Each mixture layer was packed into the column using the same tapping method, with a plastic mesh placed between each. In the middle of the three mixture layers, a resin-embedded slag fertilizer sample (diameter: 25 mm; thickness: 10 mm) containing a mirror-polished slag particle (maximum size: 1.7 mm (Food and Agriculture Materials Inspection Center, 2024) was installed. The polished surface was oriented perpendicular to the bottom of the column, allowing surface observations before and after the test. Finally, with all three soil–slag mixture layers built, the construction of the soil column leaching test apparatus and test samples (test group) was completed. As a control, columns containing six layers of soil only – without slag fertilizer and without embedded resin samples – were also prepared. For each test duration, six columns were prepared for both test and control groups. The weights of the empty column, rubber stopper, vinyl hose, plastic mesh, and gauze were measured using an electronic balance prior to packing the soil and mixtures.

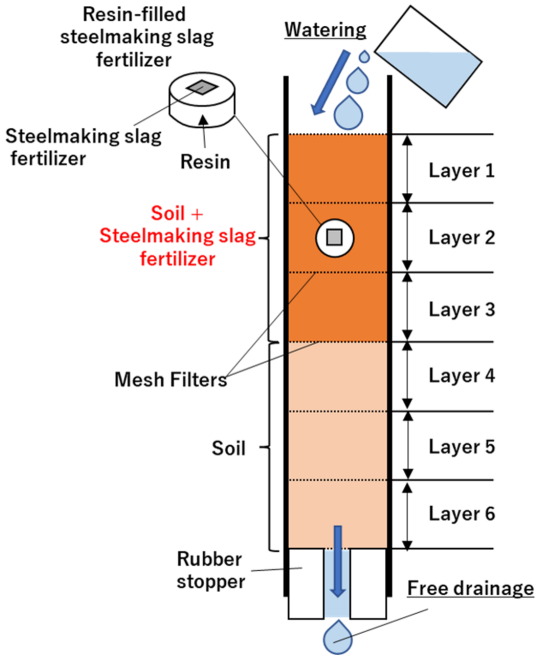

Figure 2. Schematic of experimental apparatus.

2.3 Procedure

The experimental procedure is illustrated in Fig. 3. Experimental columns packed with the samples were prepared independently for each holding period (1, 2, 4, 8, 12, and 24 weeks), with one column per period (six columns in total). In addition, for each holding period, one column was prepared for the treatment (slag fertilizer application) and one for the control, resulting in a total of 12 columns. Thus, the same columns were not monitored over time; instead, columns were collected at the endpoint of each holding period and evaluated. Each soil column containing a test sample was fixed inside an incubator maintained at 25 °C. A plastic container was placed below the vinyl hose at the bottom of the column to collect leachate. Then, 70 mL of distilled water was gently poured into the top of the column. The volume of distilled water was determined by dividing the average annual precipitation in Japan (Ministry of Land, Infrastructure, Transport and Tourism, 2006) by the number of weeks in a year. After water infiltration was complete and leachate flow from the bottom ceased, a syringe equipped with a cartridge filter (pore size: 0.2 µm) was used to collect the leachate sample. The column was then kept inside the incubator for seven days. This cycle of water addition, leachate sampling, and incubation was repeated weekly for designated durations of 1, 2, 4, 8, 12, or 24 weeks. No water was added during the final week of each experiment. To determine the water content of the soil and soil–slag mixture samples within the columns, the total weight of each column and the amount of leachate collected were measured using an electronic balance before and after water addition. After completion of the leaching tests, the columns were disassembled. The soil and soil–slag mixture layers, separated by plastic mesh, were collected layer by layer and air-dried in an incubator maintained at 40 °C for at least three days. The resin-embedded slag fertilizer samples were cleaned using an ultrasonic cleaner to remove any adhering soil and prepared for surface and cross-sectional observations.

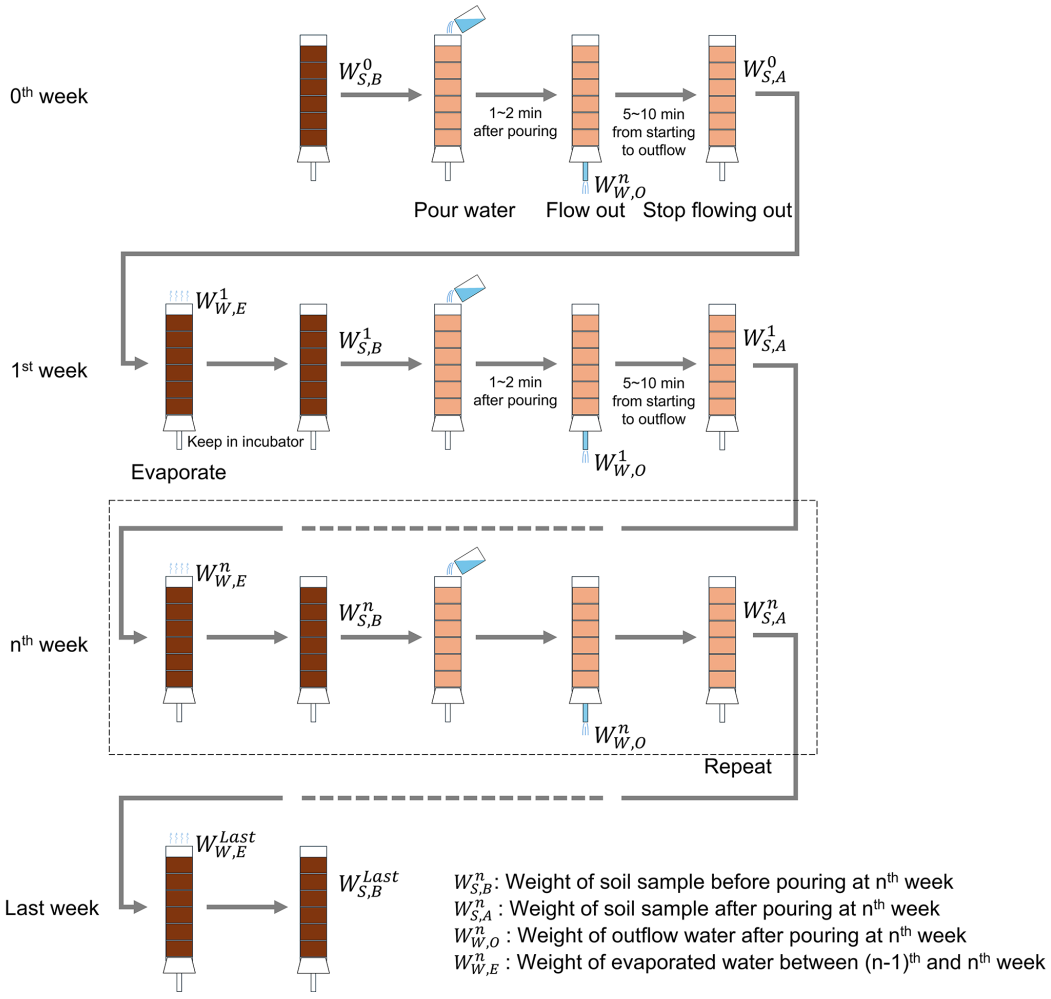

Figure 3. Experimental procedure.

2.4 Analysis

After the experiments, the soil and soil–slag mixture samples were separated layer by layer and air-dried. The dried samples were then analyzed for soil pH, exchangeable cations, and plant-available phosphorus, based on standard methods for soil and crop nutrient diagnosis (Hokkaido Research Organization, Agricultural Research Department, 2012). Soil pH was measured as follows: 20 g of the dried sample, sieved through a 2 mm mesh, was placed in a plastic bottle with 40 mL of distilled water. After stirring for approximately 30 s and allowing the mixture to settle, a pH meter was inserted into the solution and the pH value was recorded after 30 s. For the analysis of exchangeable cations, 6 g of the dried sample, also sieved through a 2 mm mesh, was placed in a plastic bottle with 120 mL of 1 N ammonium acetate solution (prepared by mixing 771 g of ammonium acetate with 9.4 L of distilled water). The mixture was shaken for 30 min using a horizontal shaker set to 160 rpm with a shaking amplitude of 40 mm. After extraction, the solution was filtered using a syringe equipped with a cartridge filter (pore size: 0.2 µm), and the concentrations of each element were measured by ICP–AES. To determine plant-available phosphorus, 3 g of the dried sample, sieved through a 0.5 mm mesh, was mixed with 600 mL of Truog's extractant (a solution prepared by mixing 30 g of ammonium sulfate, 20 mL of 1 N sulfuric acid, and 9.98 L of distilled water) in a plastic bottle. The mixture was shaken under the same conditions for 30 min and the phosphorus concentration in the extract was measured using an atomic absorption spectrophotometer. Because the measured concentrations of plant-available phosphorus were low, sampling and analysis were performed three times for each of the layer-separated samples.

The resin-embedded slag fertilizer samples were mirror-polished prior to the leaching experiments and analyzed using an electron probe microanalyzer (EPMA) equipped with a wavelength-dispersive X-ray spectrometer to obtain elemental maps and conduct quantitative analysis. To improve the accuracy of the carbon analysis, a calcium carbonate crystal was used as a standard, and calibration was performed

using a two-point calibration based on the relationship between cps and concentration, together with baseline correction. After the leaching tests, the resin-embedded samples were cleaned using an ultrasonic cleaner and air-dried, followed by additional EPMA analysis for elemental mapping and quantification. Finally, after surface analysis, each cylindrical resin-embedded sample was vertically cut, the cross-section was mirror-polished, and the same EPMA analyses were conducted on the polished cross-section.

3 Results

3.1 Temporal changes in soil pH and exchangeable CaO and MgO

Figure 4 shows the soil pH, exchangeable cations, and plant-available phosphorus measurements for each soil layer at different leaching periods. In the control columns containing only soil, soil pH remains approximately 4.8 to 5.5 across all layers. In contrast, in the test columns, the pH of the first to third layers is higher (6.0 to 6.5) compared to the control, whereas the fourth to sixth layers, which contained only soil, show pH values similar to those in the control columns. Moreover, the elevated soil pH in the first to third layers of the test columns is maintained throughout the 24-week experimental period, indicating that the pH-increasing effect of the steelmaking slag fertilizer persists over time. No increase in soil pH is observed in the fourth to sixth layers of the test columns, where the slag fertilizer was not mixed.

Focusing on the changes in exchangeable CaO and MgO resulting from the application of steelmaking slag fertilizer, the test columns show an increase of approximately 400–500 mg per 100 g of dry soil in exchangeable CaO compared to the control, while the increase in exchangeable MgO is more modest, at approximately 10–30 mg per 100 g of dry soil. A similar trend as the soil pH is observed for exchangeable CaO and MgO, with elevated levels found only in the layers containing the soil–slag mixture. In contrast to calcium and magnesium, no increase in exchangeable Na_2O and K_2O is observed over time. For exchangeable Na_2O, both the test and control columns show a trend wherein the concentrations decrease in the upper layers and increase in the lower layers over time. Plant-available phosphorus showed no substantial difference.

To compare the extent of leaching in the soil, a separate analysis was conducted using a sample in which soil and slag fertilizer were mixed but not subjected to the column leaching test; instead, the mixed sample was air-dried directly. The vertical dashed line in Fig. 4 represents the results from this control. In all cases (soil pH, exchangeable CaO, and MgO), the values are higher in the samples that underwent the column leaching test.

3.2 Surface of slag fertilizer before and after leaching

In the column leaching experiment, the same location on the surface of the resin-embedded slag fertilizer sample was observed before and after the test. Figure 5 shows secondary electron images, backscattered electron images, and elemental mapping of the resin-embedded sample before and after one week of the column leaching experiment. As the pre-experiment sample was polished, the phases constituting the slag can be clearly identified in the backscattered electron image and elemental mapping, as shown in Fig. 5a. Table 2 presents EPMA values directly measured at points 1 to 4 in Fig. 5a. In Table 2, the measured values are reported in mass % and are presented as obtained, without normalization to 100 %. Based on the elemental mapping, quantitative analysis, and the XRD pattern in Fig. 1, the mineral phases in this field of view include the C_2S phase with phosphorus solid solution; the MF phase composed of solid solutions of MgO, MnO, and FeO; the C_2F phase containing aluminum and titanium; and the f-CaO phase. In contrast to the flat surface of the pre-experiment sample, the surface after one week of leaching, as shown in Fig. 5b, can be categorized into three major morphological types. The first type consists of precipitates formed in the central and upper-right areas of Fig. 5b, which partially cover the surface of the original sample. The second type includes areas where the original surface is exposed but shows signs of cracking or surface roughening. The third type retains the original surface condition. Quantitative analysis at points 5 to 9 in Fig. 5b are shown in Table 2. Elemental mapping and the quantitative results indicate that the precipitates contain 5.3 mass % carbon, although only approximately 1 mass % was detected in the pre-experiment sample. Although surface roughening was observed on the slag fertilizer after the experiment, the resin portion remained relatively intact. The experiment was conducted largely under static conditions; therefore, the likelihood that the resin was damaged and that resin components were incorporated into the precipitates is considered low. Moreover, because the resin is highly water-resistant, incorporation into the precipitates due to dissolution and reprecipitation of the resin is also unlikely.

The phases exhibiting cracking and surface roughening are primarily composed of calcium and silicon, or are rich in calcium, corresponding to the C_2S and f-CaO phases. After one week of leaching, these phases also showed the presence of carbon. The phases that maintain their original surface conditions are the MF phase, rich in magnesium and iron; and the C_2F phase, rich in calcium, iron, and aluminum. A small portion of the C_2S phase was also observed to retain its original surface state. It should be noted that no altered phases attributable to water contact during sectioning were observed.

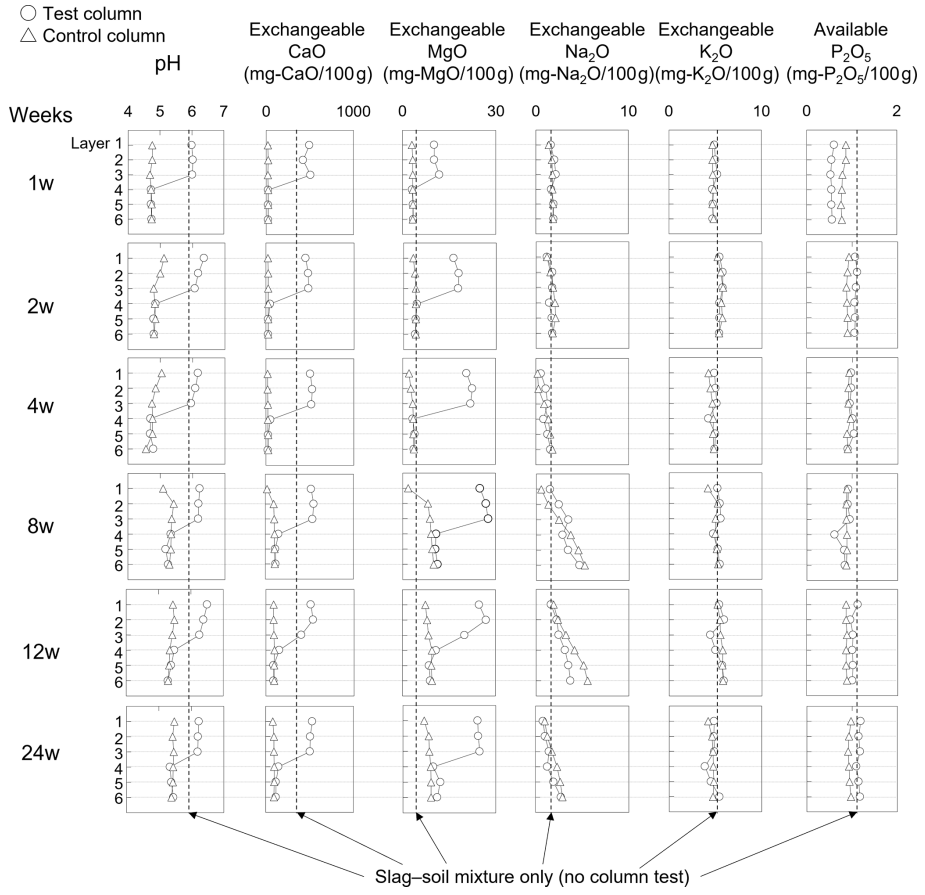

Figure 4. Results of soil elution test.

Table 2. Composition of phases before and after one week of leaching.

No.	Ca	Si	Fe	Mg	Al	P	Mn	Ti	C	O	Phase
1	40.4	11.8	0.7	0.0	0.4	3.0	0.0	0.2	1.2	30.2	C_2S
2	4.1	0.0	48.6	8.3	0.0	0.0	8.8	0.0	1.1	20.0	MF
3	29.1	0.6	23.1	0.3	5.4	0.1	0.5	4.0	1.1	25.0	C_2F
4	46.3	0.1	14.9	1.0	0.0	0.0	6.2	0.0	1.1	22.8	f-CaO
5	42.1	12.7	1.0	0.0	0.4	2.2	0.1	0.2	1.4	32.0	C_2S
6	42.1	11.8	0.8	0.0	0.4	2.0	0.1	0.1	4.8	35.8	C_2S (altered phase)
7	4.8	0.1	51.7	7.5	0.0	0.0	7.9	0.0	0.9	21.5	MF
8	29.6	0.8	23.4	0.4	4.9	0.1	0.5	4.0	1.1	25.3	C_2F
9	36.3	0.1	0.2	0.0	0.0	0.0	0.1	0.0	5.3	22.1	$CaCO_3$

3.3 Time-lapse of surface and cross-section

To examine time-dependent changes in leaching behavior, representative results of surface observations after 1, 4, 8, and 24 weeks of leaching are shown in Fig. 6. As described earlier, after one week of leaching, the precipitates partially cover the sample surface, and the dissolution of the C_2S and f-CaO phases results in cracking. After four weeks, further dissolution of these phases produces visible pits, and a broader area of the surface is covered by precipitates. The MF and C_2F phases remain unchanged, as per the observation after one week. In the sample leached for eight weeks, cracking and pitting of the C_2S and f-CaO phases are still evident. In the sample leached for 24 weeks, precipitation occurred on the slag surface has progressed further, covering the entire surface of the precipitates. In cement science, it is well known that reaction between slag components and water forms $CaO–SiO_2–H_2O$ (C–S–H) gel, and that the presence of this phase contributes to the development of mechanical strength in cementitious materials (Zhao et al., 2024). A

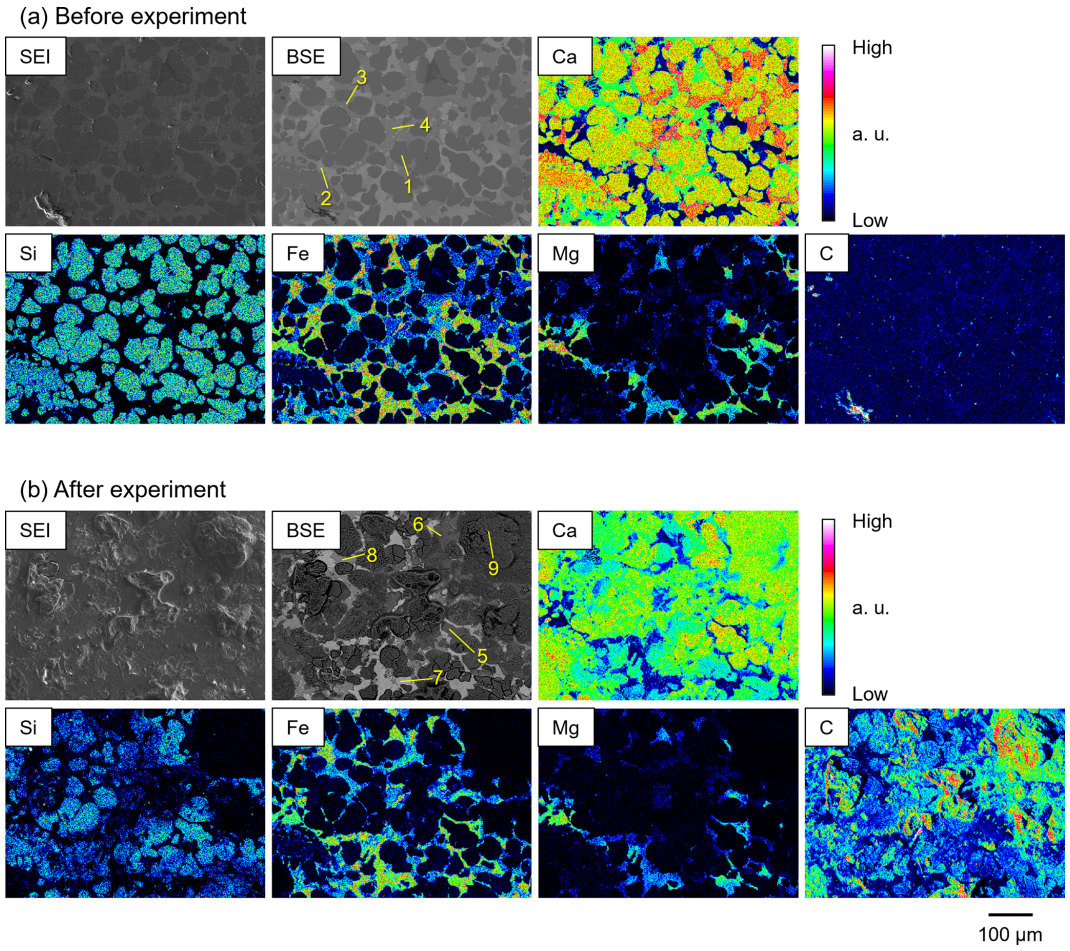

Figure 5. Surface of slag **(a)** before and **(b)** after one week of embedment.

similar reaction system may also develop in soils. However, point analyses of the surface coatings and altered layers in this study consistently detected carbon, indicating that the surface was not clearly covered by a continuous C–S–H gel layer.

Cross-sections of the samples buried for 1, 12, and 24 weeks were cut and subjected to elemental mapping of calcium and carbon, as shown in Fig. 7. The precipitation on the original polished surface of the slag is also evident in Fig. 7. In the sample leached for one week, a layer with reduced calcium concentration extending inward from the slag surface was observed, with a maximum thickness of 31 µm and an average thickness of approximately 20 µm within the observed field. Moreover, the figure shows that leaching does not progress uniformly from the surface of the slag; rather, the extent of surface erosion varies by location, indicating non-uniform leaching. This is considered to be due to the preferential dissolution of the more soluble phases such as C_2S and f-CaO, as described previously. Even after extending the leaching period to 24 weeks, the depth of erosion remains nearly unchanged, with a maximum depth of 33 µm, and a similarly non-uniform leaching front is observed as in the 1-week sample.

4 Discussion

4.1 Sources and pathways of Ca sustaining pH

Phases exhibiting cracking and surface roughening are primarily composed of calcium and silicon, or are rich in calcium, corresponding to the C_2S and f-CaO phases. In addition to cracking and roughening, surface alteration and pitting are observed on C_2S and f-CaO surfaces. After one week of leaching, precipitates containing measurable carbon are observed. Because the concentrations of elements other than Ca and O are extremely low, these precipitates are identified as $CaCO_3$. Carbon is also detected in the altered phases formed on the surfaces of C_2S and f-CaO, which is consistent with dissolution in water followed by carbonation. Taken together, these observations indicate that the f-CaO and C_2S phases in the slag are the primary sources of calcium supplied to the soil, and that dissolution of these phases progresses over time and is accompanied by increas-

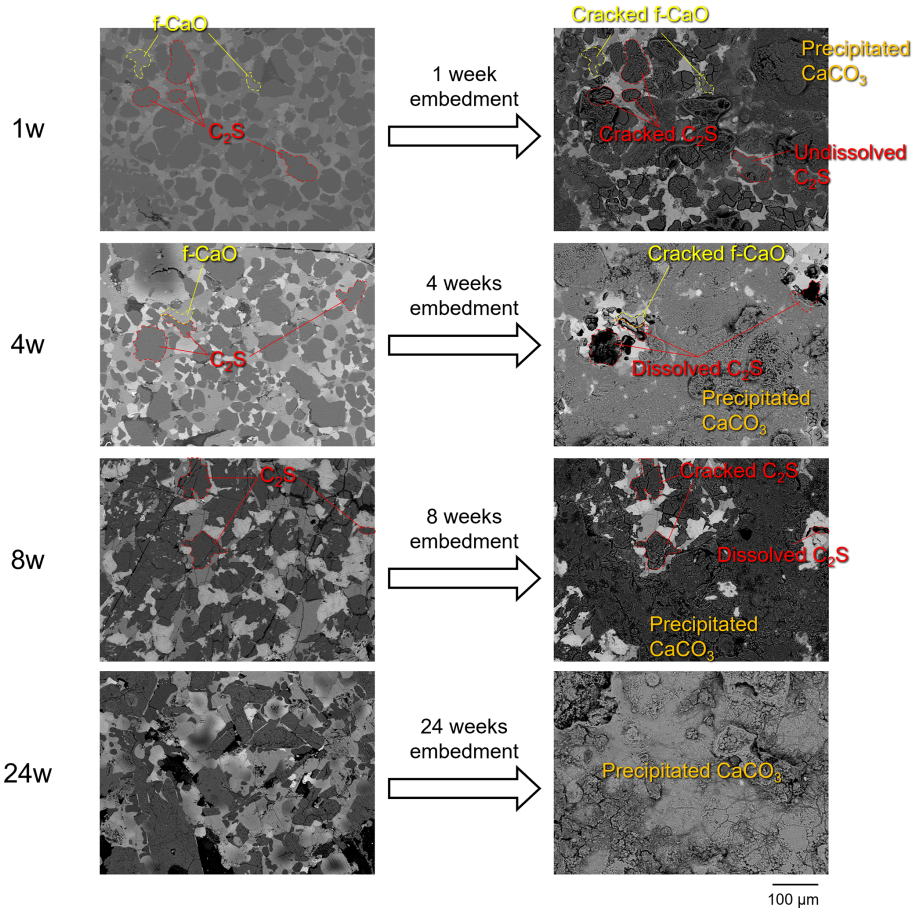

Figure 6. Surface of slags before and after 1, 4, 8, and 24 weeks of embedment.

ing precipitation of $CaCO_3$ on their surfaces. XRD analysis of the soil–slag mixture before and after the column experiment was considered to evaluate mineralogical phase changes. However, because the soil/slag mixing ratio was large, slag-derived mineral phase peaks were obscured by soil-derived peaks and did not appear clearly. Consequently, both qualitative and quantitative analyses were difficult.

The calculated solubility order shown below explains why calcium is released first from f-CaO and C_2S and subsequently retained as surface $CaCO_3$ that dissolves upon rewetting, sustaining elevated exchangeable CaO and pH.

According to previous reports (Gao et al., 2015; Futatsuka et al., 2004), the f-CaO phase and its reaction products $Ca(OH)_2$ and $CaCO_3$, as well as the C_2S phase are considered to leach into water according to Eqs. (1) to (4):

$$CaO(s) + 2H^+ = Ca^{2+} + H_2O \quad (1)$$

$$Ca(OH)_2(s) + 2H^+ = Ca^{2+} + 2H_2O \quad (2)$$

$$CaCO_3(s) + H^+ = Ca^{2+} + HCO_3^- \quad (3)$$

$$2CaO \cdot SiO_2(s) + 4H^+ = 2Ca^{2+} + {H_2SiO_3}^0 + H_2O. \quad (4)$$

Figure 8 presents pH–solubility curves for the CaO, $Ca(OH)_2$, $CaCO_3$, and C_2S phases. In these calculations, the dissolution reactions of carbon dioxide (Eqs. 5 to 7) and the dissociation reactions of the carbonate and metasilicate species (Eqs. 8 and 9) were considered (Futatsuka et al., 2004). It was assumed that the CaO, $Ca(OH)_2$, and C_2S phases dissolved while maintaining the anion-to-cation ratios as defined by their chemical composition. For $CaCO_3$, solubility was calculated under various CO_2 partial pressures. The equilibrium constants for each reaction were calculated from the chemical potentials listed in Table 3 (Barin, 1989; Chase, 1998; Futatsuka et al., 2004; Pourbaix, 1966; Pourbaix and Franklin, 1974) using the Van't Hoff isotherm.

$$H_2O + CO_2(g) = {H_2CO_3}^0 \quad (5)$$

$${H_2CO_3}^0 = H^+ + HCO_3^- \quad (6)$$

$$HCO_3^- = H^+ + CO_3^{2-} \quad (7)$$

$${H_2SiO_3}^0 = H^+ + HSiO_3^- \quad (8)$$

$$HSiO_3^- = H^+ + SiO_3^{2-} \quad (9)$$

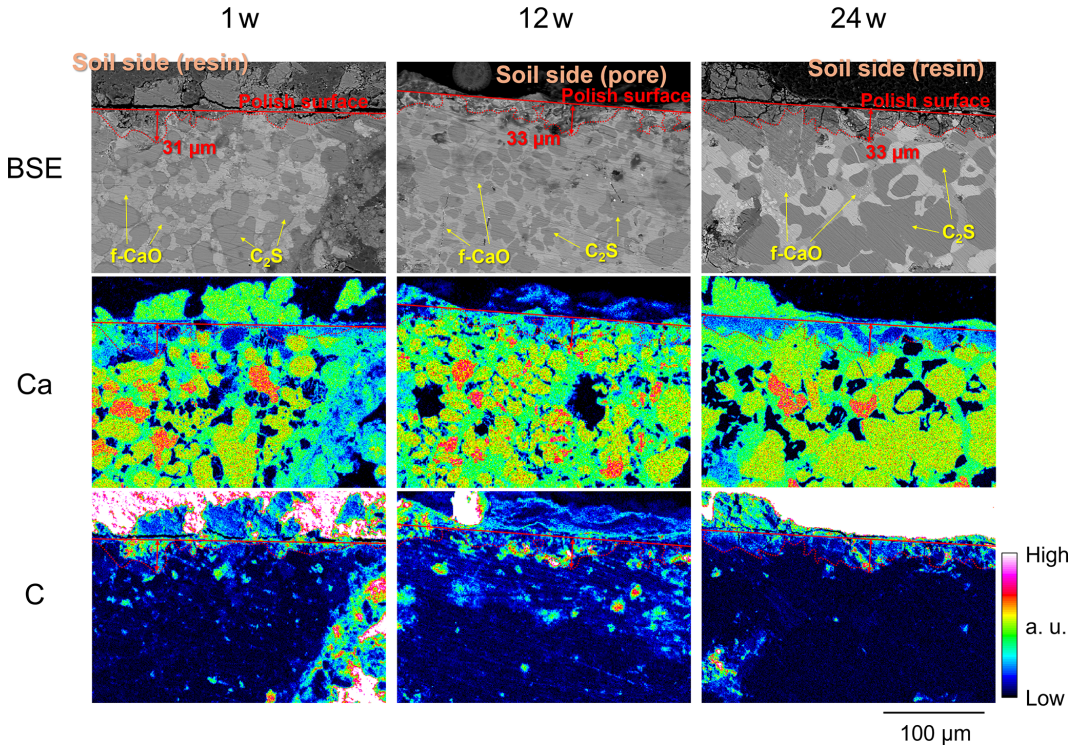

Figure 7. Cross-section of embedded slag for 1, 12, and 24 weeks.

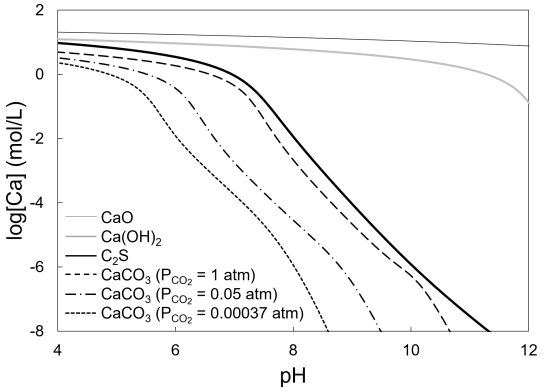

Figure 8. pH–solubility curve for calcium compounds.

Table 3. Thermodynamic data for calculation of solubility.

Chemical species	State	μ^o	Ref.
H^+	aq.	0	Pourbaix (1966)
Ca^{2+}	aq.	−553 067	Pourbaix (1966)
$H_2CO_3^0$	aq.	−624 445	Pourbaix (1966)
HCO_3^-	aq.	−587 808	Pourbaix (1966)
CO_3^{2-}	aq.	−528 129	Pourbaix (1966)
$H_2SiO_3^0$	aq.	−1 012 512	Pourbaix (1966)
$HSiO_3^-$	aq.	−955 053	Pourbaix (1966)
SiO_3^{2-}	aq.	−887 050	Pourbaix (1966)
H_2O	liq.	−237 141	Chase (1998)
CO_2	gas	−394 389	Chase (1998)
CaO	sol.	−603 592	Pourbaix and Franklin (1974)
$Ca(OH)_2$	sol.	−898 421	Chase (1998)
$2\,CaO \cdot SiO_2$	sol.	−2 198 590	Barin (1989)
$CaCO_3$	sol.	−1 128 811	Barin (1989)

The activity coefficient γ_i of chemical species i was calculated using Davies equation (Ritsema, 1993):

$$\log \gamma_i = -0.509 z_i^2 \left(\frac{\sqrt{I}}{1+\sqrt{I}} - 0.31 I \right) \quad (10)$$

$$I = \frac{1}{2} \sum_i C_i z_i^2 \quad (11)$$

where C_i and z_i are the concentration [mol L^{-1}] and charge of species i, respectively, and I is the ionic strength of the solution. From Fig. 8, it can be seen that within the soil pH range 4–7, and even at higher pH levels, phase solubility followed the sequence $CaO > Ca(OH)_2 > C_2S > CaCO_3$. Therefore, among these compounds, CaO, $Ca(OH)_2$, and the C_2S hase are readily leached, whereas $CaCO_3$ is relatively resistant to dissolution. The observed precipitates are considered to form as follows: First, Ca^{2+} ions are released from the f-CaO and C_2S phases, both of which exhibit high solubility. Since soil water is retained within soil pores, the areas near the dissolving phases experience an increase in both Ca^{2+} concentration and pH. At the elevated pH on the surface of

the slag fertilizer, Ca^{2+} ions react with bicarbonate (HCO_3^-) and carbonate (CO_3^{2-}) ions formed from the dissolution of atmospheric CO_2 into water (Eqs. 12 to 15), leading to the precipitation of $CaCO_3$.

$$CO_2(g) + H_2O = H^+ + HCO_3^- \quad (12)$$

$$Ca^{2+} + HCO_3^- = CaCO_3(s) + H^+ \quad (13)$$

$$CO_2(g) + H_2O = 2H^+ + CO_3^{2-} \quad (14)$$

$$Ca^{2+} + CO_3^{2-} = CaCO_3(s) \quad (15)$$

The cracking observed in the f-CaO and C_2S phases in this experiment is considered to be caused by their dissolution upon contact with water during infiltration, and by the volumetric expansion resulting from the formation of $Ca(OH)_2$ through the reaction of the f-CaO phase with water (Wang et al., 2010).

4.2 Ca^{2+} supply and pH enhancement under column leaching

To determine why pH and exchangeable cation levels were higher in the column samples than in those where soil and steelmaking slag fertilizer were simply mixed and dried, the following interpretation was made based on previous studies. According to a previous study in which mineral phases found in steelmaking slag were synthesized, pulverized to 53 µm or smaller, and subjected to leaching tests in a pH 5 nitric acid solution, the release of Ca^{2+} ions from C_2S continued even after 30 min (Gao et al., 2015). In the present study, slag fertilizer with a larger particle size was used, suggesting that the 30-minute shaking period used for the analysis of pH and exchangeable cations may not have been sufficient to complete the release of Ca^{2+} ions. Furthermore, the release of Ca^{2+} and Mg^{2+} ions from the slag promotes ion exchange with H^+ ions adsorbed onto the soil surface, displacing them into the pore water. These H^+ ions are then either flushed out of the system by water infiltration or neutralized by OH^- ions generated during the slag dissolution process, which in turn increases the soil pH. Therefore, the observed increase in pH and exchangeable cation concentrations in the column samples is likely attributable to the extended reaction time within the column during the leaching period. On the other hand, previous studies (Gao et al., 2015; Iwama et al., 2020) have reported that the MF phase and the C_2F phase are resistant to leaching, which is consistent with the present observation that these phases maintain their original surface condition where exposed.

4.3 Agronomic implications

Taken together with the solubility-based analysis, observations of slag surfaces and cross-sections suggest that the increase in soil pH reflects dissolution of alkaline components. In addition to the Ca^{2+} and Mg^{2+} that leach from the slag and become adsorbed onto soil particle surfaces, some of the extracted amounts likely originate from CaO and MgO contained in the slag fertilizer itself, as well as from precipitates formed during the leaching experiment. $CaCO_3$ is known to dissolve gradually in soil and provide a sustained increase in pH. Therefore, the long-term effectiveness of steelmaking slag fertilizer in improving soil pH may be attributed to its continuous supply of $CaCO_3$ to the soil. This precipitation of $CaCO_3$ helps retain calcium near the slag particles over an extended period, maintaining elevated levels of both soil pH and exchangeable CaO for at least 24 weeks. In the 24-week leaching tests, the depth of the altered layer did not show a marked increase with time. In contrast, under longer-term conditions where re-dissolution of $CaCO_3$ in the surface layer could proceed, or under field conditions involving plant roots – where organic acids released from roots may decrease pH and plants may take up Ca-bearing nutrients – the erosion front of the slag fertilizer is expected to gradually advance into the interior through readily soluble phases (f-CaO and C_2S), given that a robust, single-phase C–S–H coating was not formed. The liming effect would diminish once water can no longer access these readily soluble phases. In other words, if manufacturing processes are designed to promote growth of these readily soluble phases or if crushing is intensified to increase their exposure, the CaO component in slag fertilizer may be utilized more effectively. Both the downward movement of this fertilizer effect within the soil profile and runoff from upland fields are very small. This, in turn, suggests that the steelmaking slag fertilizer must be incorporated into the soil to the depth at which the effect is required to achieve soil pH improvement.

Since calcium and magnesium exhibit antagonistic interactions, where an excess of one can inhibit the uptake of the other, the desirable ratio of exchangeable CaO to exchangeable MgO in Japanese soils is considered to be approximately 65–75 : 20–25 in molar terms (Minister of Agriculture, Forestry and Fisheries, 2008). Given that the observed increases are approximately 400–500 to 10–30 mg per 100 g of dry soil, the application of steelmaking slag fertilizer results in an excess of calcium. Therefore, it is advisable to apply a supplemental magnesium source depending on soil type and the crop being cultivated.

Because no replicate column experiments were performed in this study, it is not possible to draw a definitive conclusion as to whether the presence or absence of slag fertilizer application affects plant-available phosphorus. Nevertheless, previous studies have reported an increase in soil phosphorus concentration following steelmaking slag application (Deus et al., 2020). One possible reason why no clear difference was observed here is the difference in soil type. Because an Andosol, which has a higher phosphorus adsorption capacity than an Oxisol (Osorio and Habte, 2015), was used in this study, the improvement effect associated with liming (including slag application) may have differed from that reported for Oxisols in the literature.

4.4 Upland vs. paddy: unique carbonation

Although the dissolution of the C_2S phase has been previously observed in experiments simulating paddy field conditions (Ito, 2022), precipitation of the $CaCO_3$ phase on the slag surface has not been reported.

In upland-type settings, repeated wetting and drying generate short periods of high pH and high Ca^{2+} concentration near dissolving slag particles. Aeration ensures a continuous CO_2 supply, while pore-scale water retention prolongs contact between porewater and reactive surfaces. These environmental conditions favor local supersaturation with respect to calcite, so thin $CaCO_3$ skins form and thicken over time. By contrast, during continuous flooding, gas exchange is strongly suppressed and the supply of CO_2 to the soil solution is limited. Because wet–dry cycles are absent, supersaturation with respect to $CaCO_3$ is less likely and carbonate skins on slag surfaces are unlikely to form. This pattern appears to be characteristic of upland environments. From a management perspective, when long-term pH persistence via $CaCO_3$ cycling is desired, practices that allow intermittent drying and good aeration are advantageous. In continuously flooded systems, this mechanism is expected to weaken.

4.5 Mechanism of slag fertilizer leaching in soil

The leaching behavior of steelmaking slag fertilizer in soil under repeated wetting and drying conditions is inferred as illustrated in Fig. 9. First, infiltrating water reacts with and dissolves the C_2S and f-CaO phases. Simultaneously, water retained within the slag gradually penetrates these phases. The Ca^{2+} ions released through dissolution are partially transported away with migrating water, whereas the remaining Ca^{2+} ions within water retained in the soil react with the CO_3^{2-} ions formed by the dissolution and ionization of atmospheric CO_2, resulting in the formation of a $CaCO_3$ phase on the slag surface. Furthermore, CO_2 also dissolves into the water that has infiltrated the slag body, where it reacts with the C_2S and f-CaO phases to form altered phases. At the earliest stage, highly reactive f-CaO and C_2S phases are exposed in the slag, and cross-sectional observations suggest that the leaching depth is determined primarily by the initial slag–water reaction that occurs immediately after application. Subsequently, the newly infiltrated water dissolves both the previously precipitated $CaCO_3$ phase and the altered phase, thereby supplying further Ca^{2+}. This cycle of $CaCO_3$ precipitation and dissolution of both the altered and $CaCO_3$ phases is then repeated. Although the altered phase includes components that have reacted with CO_2, it mainly consists of the highly soluble C_2S and f-CaO phases, whose dissolution continues preferentially. As the leaching period is extended, this process manifests as the formation of pits. Because the $CaCO_3$ phase has lower solubility than the C_2S and f-CaO phases, Ca^{2+} released from these phases reacts with atmospheric CO_2 and precipitates as $CaCO_3$. Consequently, the surface coverage of $CaCO_3$ increases with prolonged leaching. Even after 24 weeks, a substantial amount of unreacted C_2S and f-CaO phases remain inside the particles, along with residual precipitated $CaCO_3$ on the surface. This indicates that the potential for calcium release from the slag remains well preserved at this stage. Figure 6 indicates that $CaCO_3$ has the lowest solubility among the calcium salts. In addition, highly soluble CaO and C_2S phases remaining within the slag may increase the local pH and thereby retard the dissolution of $CaCO_3$. However, the experimental results showed that, even at 24 weeks, the exchangeable CaO content still remained high. These findings suggest that, while the soil-improvement effect is maintained, leaching of calcium components by rainfall or irrigation is suppressed, and thus the long-term manifestation of the effect can be expected. At 24 weeks, no robust coating of C–S–H gel was observed, suggesting that the cycle of f-CaO and C_2S dissolution, $CaCO_3$ precipitation, and subsequent re-dissolution of $CaCO_3$ is still maintained.

The leaching behavior of Mg may follow a pathway different from that of Ca. Formation of an $MgCO_3$ phase and incorporation of Mg into the $CaCO_3$ phase were not observed in this study. In addition, because $MgCO_3$ is difficult to precipitate due to the high hydration activity of Mg^{2+}, carbonate formation is unlikely to be a dominant pathway. Instead, the slag fertilizer may contain Mg-bearing phase(s) that are poorly soluble in water but readily soluble in ammonium acetate extract, which could explain the persistently high exchangeable MgO. Such a form may suppress Mg loss by rainfall or watering while providing plant nutrition over a long period, analogous to the behavior inferred for Ca. As a candidate mineral phase supplying Mg in the slag fertilizer, the MF phase, which contains a relatively high MgO content according to the quantitative analysis in Table 2, is proposed. In addition, based on the phase compositions and leaching behaviors, it is likely that phosphate is supplied from the C_2S phase, and that the trace essential elements iron and manganese are supplied from the f-CaO phase.

4.6 Challenges for expanding the scope of application

4.6.1 Changes under long-term application

In this study, the column leaching test was terminated at 24 weeks. Based on the experimental results, it is expected that the soil pH correction capacity would be maintained even if a leaching test were conducted for a longer period. If the consumption process of the slag fertilizer can be continuously observed and the consumption rate can be quantified, this would contribute to improving fertilizer application design.

4.6.2 Effects on plant-available phosphorus

In this study, no significant change in plant-available phosphorus was observed. On the other hand, previous studies

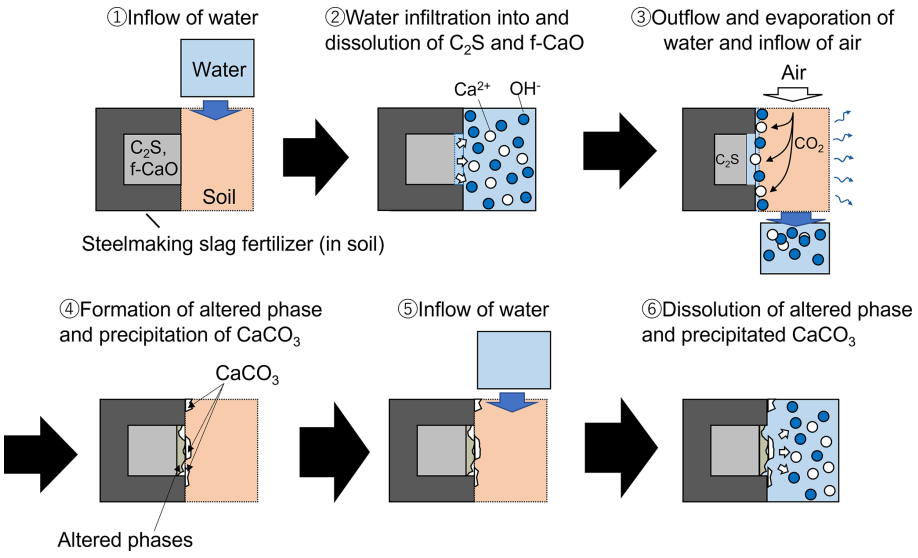

Figure 9. Elution behavior of slag fertilizer in soil.

have reported an increase in plant-available phosphorus. Possible reasons why no difference was detected in this study include both the possibility that the statistical power was insufficient due to the small number of replicates and the possibility that the actual effect is small (or does not appear under certain conditions). Therefore, additional experiments with an increased number of replicates are needed for statistical verification.

4.6.3 Evaluation of the leaching potential of heavy metals

This study did not evaluate the leaching behavior of heavy metals because the product used is one for which it was confirmed in advance – based on the guidelines of the Nippon Slag Association – that the contents and leaching amounts of harmful heavy metals do not pose a problem. Although many reports suggest that the impact of heavy metals is small, it remains a concern. By first identifying the partitioning of heavy metals among the respective mineral phases and then applying the approach used in this study, it would be possible to estimate the amount that could leach when the material is applied to soil.

4.6.4 Expression of fertilizer effects under crop cultivation conditions

As described in the background, in actual crop production environments, leaching behavior may change due to complex interactions in the rhizosphere. By conducting tests while cultivating crops in a similar experimental system, it is possible to evaluate the effects of the presence of plants on the consumption and leaching behavior of the slag fertilizer by comparison with non-cultivated conditions.

5 Conclusion

To investigate the mechanisms of soil pH improvement and component leaching of slag fertilizer under upland conditions, a leaching test was conducted using a soil column system simulating an upland agricultural environment. The following conclusions are drawn from the results:

- In the control columns, soil pH remained approximately 4.8–5.5 throughout the experimental period. In contrast, in the test columns, the soil layers containing slag maintained a pH of 6.0–6.5, which remained stable without declining over the 24-week study period.

- Exchangeable CaO and MgO levels were higher in the slag-mixed layers of the test columns and were similarly maintained at elevated levels for 24 weeks.

- The f-CaO and C_2S phases contained in the slag were found to dissolve, and $CaCO_3$ precipitates formed on the slag surfaces. With longer leaching duration, the f-CaO and C_2S phases exhibited progressive dissolution, resulting in the formation of pits, while the surface coverage of $CaCO_3$ increased.

- Even after 24 weeks of leaching, the f-CaO and C_2S phases remained within the slag, and $CaCO_3$ deposits remained on the slag surface.

These findings demonstrate that fertilizer derived from steelmaking slag can provide sustained improvement in soil pH. The sustained release of calcium from the f-CaO and C_2S phases, along with the precipitation of $CaCO_3$, contributes to maintaining this effect over a period of at least 24 weeks. These results not only support the potential use of

steelmaking slag fertilizer in upland agriculture but also suggest its added value and broader applicability as a recycled fertilizer material. In addition, this setup could be adapted, as needed, to quantify the partitioning of applied elements among the root-zone, subsoil, and outflow.

Data availability. The datasets are available in the Tohoku University Repository (https://doi.org/10.50974/0002007606, Iwama et al., 2026).

Author contributions. Conceptualization: TI, SK, MO and SU. Data curation: TI and MO. Formal analysis: TI and SK. Investigation: TI and MO. Methodology: TI, SK and MO. Project administration: TI, SK and SU. Resources: SK and SU. Supervision: SU. Validation: TI, SK, MO and SU. Visualization: TI and SK. Writing (original draft preparation): TI and SK. Writing (review and editing): TI, SK, MO and SU.

Competing interests. The contact author has declared that none of the authors has any competing interests.

Disclaimer. Publisher's note: Copernicus Publications remains neutral with regard to jurisdictional claims made in the text, published maps, institutional affiliations, or any other geographical representation in this paper. The authors bear the ultimate responsibility for providing appropriate place names. Views expressed in the text are those of the authors and do not necessarily reflect the views of the publisher.

Review statement. This paper was edited by Rafael Clemente and reviewed by Ian Burke and one anonymous referee.

References

Ahire, M. L., Mundada, P. S., Nikam, T. D., Bapat, V. A., and Penna, S.: Multifaceted roles of silicon in mitigating environmental stresses in plants, Plant Physiol. Biochem., 169, 291–310, https://doi.org/10.1016/j.plaphy.2021.11.010, 2021.

Alcarde, J. C. and Rodella, A. A.: Quality and legislation of fertilizers and soil amendments (in Portuguêse), Top. Ciênc. Solo (Top. Soil Sci.), 3, 291–334, 2003.

Amoakwah, E., Shim, J., Kim, S., Lee, Y., Kwon, S., Sangho, J., and Park, S.: Impact of silicate and lime application on soil fertility and temporal changes in soil properties and carbon stocks in a temperate ecosystem, Geoderma, 433, 116431, https://doi.org/10.1016/j.scitotenv.2017.08.020, 2023.

Appelo, C. A. J. and Postma, D.: Geochemistry, Groundwater and Pollution, in: 2nd Edn., CRC Press, London, ISBN 9780415364287, 2004.

Barin, I.: Thermochemical data of pure substances, VCH, New York, ISBN 089573866X, 1989.

Caires, E. F., Blum, J., Barth, G., Garbuio, F. J., and Kusman, M. T.: Changes in chemical soil characteristics and soybean response to lime and gypsum applications in a no-tillage system (in Portuguêse), R. Bras. Ci. Solo (Braz. J. Soil Sci.), 27, 275–286, https://doi.org/10.1590/S0100-06832003000200008, 2003.

Castro, G. S. A., Calonego, J. C., and Crusciol, C. A. C.: Soil physical properties in crop rotation systems as affected by liming materials (in Portuguêse), Pesqui. Agropecu. Bras. (Braz. Agric. Res.), 46, 1690–1698, https://doi.org/10.1590/S0100-204X2011001200015, 2011.

Chase, M. W. (Ed.): NIST-JANAF Thermochemical Tables, in: 4th Edn., Monograph 9, American Institute of Physics, ISBN 1563968312, 1998.

Das, B., Prakash, B., Reddy, P. S. R., and Misra, V.: An overview of utilization of slag and sludge from steel industries, Resour. Conserv. Recycl., 50, 40–57, https://doi.org/10.1016/j.resconrec.2006.05.008, 2007.

Deus, A. C. F., Büll, L. T., Guppy, C. N., Santos, S. M. C., and Moreira, L. Q. M.: Effects of lime and steel slag application on soil fertility and soybean yield under a no til-system, Soil Till. Res., 196, 104422, https://doi.org/10.1016/j.still.2019.104422, 2020.

EU – steel slags as liming materials on soil fertility, crop yields and plant health (SLAGFERTILISER), https://op.europa.eu/en/publication-detail/-/publication/af62312a-024b-11e7-8a35-01aa75ed71a1 (last access: 5 March 2026), 2017.

Food and Agriculture Materials Inspection Center: To establish official standards for ordinary fertilizers in accordance with the Law Concerning Assurance of Fertilizer Quality, etc., http://www.famic.go.jp/ffis/fert/kokuji/60k0284.pdf, (last access: 5 September 2025), 2024.

Furuzono, S., Hidaka, H., and Yamashita, K.: A simplified method for evaluating available silica in siliceous materials using the reciprocating shake extraction method with neutral Tris buffer, Nippon Dojo-Hiryogaku Zasshi (Jpn. J. Soil Sci. Plant Nutr.), 93, 392–397, https://doi.org/10.20710/dojo.93.6_392, 2022.

Futatsuka, T., Shitogiden, K., Miki, T., Nagasaka, T., and Hino, M.: Dissolution behavior of nutrition elements from steelmaking slag into seawater, ISIJ Int., 44, 753–761, https://doi.org/10.2355/isijinternational.44.753, 2004.

Gao, X., Maruoka, N., Kim, S. J., Ueda, S., and Kitamura, S.: Dissolution behavior of nutrient elements from fertilizer made of steelmaking slag, in an irrigated paddy field environment, J. Sustain. Metal., 1, 304–313, https://doi.org/10.1007/s40831-015-0030-8, 2015.

Goto, I.: Development and promotion of agricultural utilization technology for converter slag, Shokubutsu-Boeki (Plant Prot.), 70, 209–214, 2016.

Goulding, K. W. T.: Soil acidification and the importance of liming agricultural soils with particular reference to the United Kingdom, Soil Use Manage., 32, 390–399, https://doi.org/10.1111/sum.12270, 2016.

Gu, W. F., Diao, J., Tao, H. R., Deng, J. Y., Yu, H. F., Iwama, T., Cheremisina, E., Li, H. Y., Xie, B., and Ueda, S.: Effects of cooling methods on phase evolution, microstructure, and stability of steelmaking slag, Metal. Mater. Trans. B, 56, 3970–3979, https://doi.org/10.1007/s11663-025-03618-4, 2025.

Hokkaido Research Organization, Agricultural Research Department: Analytical methods for soil and crop nutrition diagnos-

tics 2012, https://www.hro.or.jp/upload/13651/0.pdf (last access: 5 September 2025), 2012.

Holland, J. E., Bennett, A. E., Newton, A. C., White, P. J., McKenzie, B. M., George, T. S., Pakeman, R. J., Bailey, J. S., Fornara, D. A., and Hayes, R. C.: Liming impacts on soils, crops and biodiversity in the UK: A review, Sci. Total Environ., 610–611, 316–332, https://doi.org/10.1016/j.scitotenv.2017.08.020, 2018.

Inubushi, K.: Sustainable soil management in East, South and Southeast Asia, Soil Sci. Plant Nutr., 67, 1–9, https://doi.org/10.1080/00380768.2020.1835431, 2021.

Inubushi, K., Saito, H., Arai, H., Ito, K., Endoh, K., and Yashima, M. M.: Effect of oxidizing and reducing agents in soil on methane production in Southeast Asian paddies, Soil Sci. Plant Nutr., 64, 84–89, https://doi.org/10.1080/00380768.2017.1401907, 2018.

Ito, K.: Suppression of methane gas emission from paddy fields, Tech. Rep. 109, Nippon Steel and Sumitomo Metal, 145–148, https://www.nipponsteel.com/en/tech/report/nssmc/pdf/109-25.pdf (last access: 5 September 2025), 2015.

Ito, K.: Elution of plant nutrition elements from steel slag fertilizers in a paddy field, Tech. Rep. 127, Nippon Steel, 100–108, https://www.nipponsteel.com/en/tech/report/pdf/127-17.pdf (last access: 5 September 2025), 2022.

Ito, K., Endoh, K., Shiratori, Y., and Inubushi, K.: Silicon elution from three types of steel slag fertilizers in a paddy field analyzed by electron probe micro-analyzer (EPMA), Soil Sci. Plant Nutr., 61, 835–845, https://doi.org/10.1080/00380768.2015.1064326, 2015.

Iwadate, Y.: Reducing soil-borne disease damage through soil pH improvement using converter slag, Tsuchidukuri-to-Ekonogyo (Soil Manage. Eco-Friendly Agric.), 49, 42–47, 2017.

Iwama, T., Du, C. M., Koizumi, S., Gao, X., Ueda, S., and Kitamura, S. Y.: Extraction of phosphorus and recovery of phosphate from steelmaking slag by selective leaching, ISIJ Int., 60, 400–407, https://doi.org/10.2355/isijinternational.ISIJINT-2019-298, 2020.

Iwama, T., Koizumi, S., Obara, M., and Ueda, S.: Raw data_Leaching Behavior of Steelmaking Slag Fertilizer under Repeated Wetting and Drying Conditions Simulating Upland Soil, Tohoku Univ. Repos. [data set], https://doi.org/10.50974/0002007606, 2026.

JOGMEC: Mineral resources material flow, 27. Phosphorus, https://mric.jogmec.go.jp/wp-content/uploads/2023/03/material_flow2021_P.pdf (last access: 5 September 2025), 2021.

Li, G., Liu, P., Chao, S., Zhang, X., Li, J., Zhang, Y., and Duan, Y.: The mineral phase evolution characteristics and hydration activity enhancement mechanism of steel slag under NaOH alkaline excitation, J. Alloys Compd., 978, 173524, https://doi.org/10.1016/j.jallcom.2024.173524, 2024.

Maruoka, N., Okubo, M., Shibata, H., Gao, X., Ito, T., and Kitamura, S.: Improvement of desalted paddy soil by the application of fertilizer made of steelmaking slag (Recovery of a paddy field damaged by the tsunami using fertilizer made of steelmaking slag-1), Tetsu-to-Hagané, 101, 445–456, https://doi.org/10.2355/tetsutohagane.TETSU-2014-131, 2015.

Matsubae-Yokoyama, K., Kubo, H., Nakajima, K., and Nagasaka, T.: A material flow analysis of phosphorus in Japan, J. Ind. Ecol., 13, 687–705, https://doi.org/10.1111/j.1530-9290.2009.00162.x, 2009.

Matsui, S.: Stabilization of calcium compounds in steelmaking slag, Tech. Rep. 125, Nippon Steel, 93–98, https://www.nipponsteel.com/en/tech/report/pdf/125-17.pdf (last access: 5 September 2025), 2020.

Minister of Agriculture, Forestry and Fisheries: Publication of basic guidelines for geo-enhancement, https://www.maff.go.jp/j/seisan/kankyo/hozen_type/h_dozyo/pdf/chi4.pdf (last access: 5 September 2025), 2008.

Ministry of Land, Infrastructure, Transport and Tourism: Rivers in Japan, https://www.mlit.go.jp/river/basic_info/english/pdf/riversinjapan.pdf (last access: 5 September 2025), 2006.

Murakami, K. and Goto, I.: Control of clubroot disease in Brassica vegetables through high application of converter slag, Agric. Hortic., 81, 445–452, 2006.

NARO – National Agriculture and Food Research Organization: Damage reduction techniques for soilborne Fusarium disease by correcting soil pH with converted slag as a core technology, research results, https://www.naro.go.jp/publicity_report/publication/archive/files/tenro-slag-2.pdf (last access: 5 September 2025), 2015.

Nippon Slag Association: Characteristics and usefulness of steel slag products, https://www.slg.jp/cms/wp-content/themes/original/pdf/pamph-sustainability_2015.pdf (last access: 5 September 2025), 2015.

Nippon Slag Association: Overview of steel slag supply and demand in FY2023, https://www.slg.jp/cms/wp-content/themes/original/pdf/report-2023-01.pdf (last access: 5 March 2026), 2024.

Nippon Slag Association: Guidelines for the Management of Steel Slag Products, https://www.slg.jp/cms/wp-content/themes/original/pdf/guideline_20260115.pdf (last access: 5 March 2026), 2026.

Okubo, M., Maruoka, N., Shibata, H., Gao, X., Ito, T., and Kitamura, S.: Long-term dissolution characteristics of various fertilizers made of steelmaking slag in a desalted paddy soil environment (Recovery of a paddy field damaged by the tsunami using fertilizer made of steelmaking slag-2), Tetsu-to-Hagané, 101, 457–464, https://doi.org/10.2355/tetsutohagane.TETSU-2014-132, 2015.

Oliveira, E. L. and Pavan, M. A.: Control of soil acidity in no-tillage system for soybean production, Soil Till. Res., 38, 47–57, https://doi.org/10.1016/0167-1987(96)01021-5, 1996.

Osorio, N. W. and Habte, M.: Effect of a phosphate-solubilizing fungus and an arbuscular mycorrhizal fungus on leucaena seedlings in tropical soils with contrasting phosphate sorption capacity, Plant Soil, 389, 375–385, https://doi.org/10.1007/s11104-014-2357-5, 2015.

Pistocchi, C., Ragaglini, G., Colla, V., Branca, T. A., Tozzini, C., and Romaniello, L.: Exchangeable Sodium Percentage decrease in saline sodic soil after Basic Oxygen Furnace Slag application in a lysimeter trial, J. Environ. Manage., 203, 896–906, https://doi.org/10.1016/j.jenvman.2017.05.007, 2017.

Pourbaix, M.: Atlas of Electrochemical Equilibria, Pergamon Press, Oxford, ISBN 10 0080109853, 1966.

Pourbaix, M. and Franklin, J. A.: Atlas of electrochemical equilibria in aqueous solutions, in: 2nd Edn., National Association of Corrosion Engineers, Houston, ISBN 10 0915567989, 1974.

Ritsema, C. J.: Estimation of activity coefficients of individual ions in solutions with ionic strengths up to 0.3 mol dm^{-3},

Eur. J. Soil Sci., 44, 307–315, https://doi.org/10.1111/j.1365-2389.1993.tb00454.x, 1993.

Saigusa, M. and Matsuyama, N.: Distribution of allophanic andosols and non-allophanic andosols in Japan, Tohoku J. Agricul. Res., 48, 75–83, 1998.

Shiratori, Y.: Development of methane emission control measures for rice paddy fields and visualization technology for hydrogen sulfide, Hiryo-Kagaku (Fert. Sci.), 46, 73–97, 2024.

Sinegovskaya, V. T., Banetskaya, E. V., Boiarskii, B. S., Sinegovskii, M. O., and Nikulchev, K. A.: Role of soil liming in increasing crop yields in crop rotation, IOP Conf. Ser.: Earth Environ. Sci., 547, 012037, https://doi.org/10.1088/1755-1315/547/1/012037, 2020.

Verma, K. K., Song, X. P., Liang, Q., Huang, H. R., Bhatt, R., Xu, L., Chen, G. L., and Li, Y. R.: Unlocking the role of silicon against biotic stress in plants, Front. Plant Sci., 15, 1430804, https://doi.org/10.3389/fpls.2024.1430804, 2024.

Wang, G., Wang, Y., and Gao, Z.: Use of steel slag as a granular material: volume expansion prediction and usability criteria, J. Hazard. Mater., 184, 555–560, https://doi.org/10.1016/j.jhazmat.2010.08.071, 2010.

Yamamoto, S. and Morii, H.: Suppression of methane production via the promotion of Fe^{2+} oxidation in paddy fields, Commun. Soil Sci. Plant Anal., 51, 1114–1122, https://doi.org/10.1080/00103624.2020.1751192, 2020.

Zhao, J., Li, Z., Zhu, H., Liu, Q., and Liu, J.: Dissolution-precipitation hydration mechanism of steel slag based on ion exchange of a layered alkali-activator, Constr. Build. Mater., 411, 134795, https://doi.org/10.1016/j.conbuildmat.2023.134795, 2024.